

# Energy carriers in the Fermi-Pasta-Ulam $\beta$ lattice: Solitons or Phonons?

N. Li,<sup>1</sup> B. Li,<sup>2,3</sup> and S. Flach<sup>1</sup>

<sup>1</sup>*Max Planck Institute for the Physics of Complex Systems,  
Nöthnitzer Strasse 38, D-01187 Dresden, Germany*

<sup>2</sup>*NUS Graduate School for Integrative Sciences and Engineering, Singapore 117456, Republic of Singapore*

<sup>3</sup>*Department of Physics and Centre for Computational Science and Engineering,  
National University of Singapore, Singapore 117546, Republic of Singapore*

(Dated: February 28, 2022)

We investigate anomalous energy transport processes in the Fermi-Pasta-Ulam  $\beta$  lattice. They are determined by the maximum sound velocity of the relevant weakly damped energy carriers. That velocity can be numerically resolved by measuring the propagating fronts of the correlation functions of energy/momentum fluctuations at different times. The numerical results are compared with the predictions for solitons and effective (renormalized) phonons, respectively. Excellent agreement has been found for the prediction of effective long wavelength phonons, giving strong evidence that the energy carriers should be effective phonons rather than solitons.

PACS numbers: 05.45.-a,05.60.-k

Energy transport in low dimensional systems has attracted enduring interest [1–4]. One striking finding is the phenomenon of anomalous transport [5–7], which has recently been experimentally verified for carbon nanotubes [8]. Theoretical efforts [2, 9, 10] usually follow the pioneering work of Peierls and focus on the low temperature region, where weakly interacting phonons are considered to be the responsible energy carriers. A microscopic transport theory beyond the low temperature regime is still lacking, which leaves the explanation for most existing numerical and experimental results far from satisfactory. One central question concerns the type of energy carriers whose properties determine the underlying transport behavior at higher temperatures. As temperature or nonlinearity is increased, collective motions other than phonons could also be excited. It is thus desirable to identify the specific energy carriers for these low dimensional systems.

The Fermi-Pasta-Ulam  $\beta$  (FPU- $\beta$ ) lattice is a classic example showing the effect of anomalous transport, and therefore a perfect testbed for comparison between theoretical predictions and numerical experiments. Anomalous transport manifests through an increase of the heat conductivity with the system size. This in turn implies that the responsible energy carriers are anomalously weakly damped and propagate “ballistically” over very long distances. Due to nonlinearity, solitons [11, 12], discrete breathers [13] and interacting phonons [14–18] are candidates for these carriers. In particular, supersonic solitons have been considered as major energy carriers which are responsible for the anomalous transport behavior [19, 20]. The pivotal evidence supporting the idea of soliton transport is the numerical observation of ultrasonic energy transfer. The sound velocity  $c_s$  of energy transfer was measured by following the spreading of an initial energy pulse, using both non-equilibrium [19, 21] and equilibrium [20] methods. In particular, the temperature-dependent sound velocity  $c_s$  is compared with a prediction derived from soliton theory [12] and

good agreement has been found in Ref. [19]. However, strong finite size effects of the soliton velocities were not clarified in Ref. [12]. The same data for  $c_s$  in Ref. [19] are also in good agreement with the predicted velocity for effective phonons [17]. The uncertainty of the computed data in Ref. [19] is too large to distinguish between the two predictions. To identify the true energy carriers, a more accurate numerical determination of  $c_s$  is needed.

In the present paper, we apply the equilibrium approach recently developed by Zhao [20] to study the energy transport properties in the FPU- $\beta$  lattice. As demonstrated in Ref. [20], the sound velocities  $c_s$  can be measured with very high precision. We will show that the numerical results are in very good agreement with the prediction for effective phonons and the agreement is not limited to the FPU- $\beta$  lattice. The soliton predictions show clear deviations and can be ruled out.

We consider the dimensionless Hamiltonian for the FPU- $\beta$  lattice

$$H = \sum_{i=1}^N \left[ \frac{p_i^2}{2} + \frac{1}{2}(q_i - q_{i-1})^2 + \frac{1}{4}(q_i - q_{i-1})^4 \right] \quad (1)$$

where  $p_i$  denotes the momentum and  $q_i$  denotes the displacement from equilibrium position for the  $i$ -th atom with  $i = 0, \pm 1, \pm 2, \dots, \pm N/2$ . The local energy density is defined as  $H_i = p_i^2/2 + (q_i - q_{i-1})^2/2 + (q_i - q_{i-1})^4/4$ . Fixed boundary conditions are applied to the two end atoms, which are additionally coupled to stochastic Langevin heat baths with specified temperature  $T$ . The normalized correlation functions of energy and momentum fluctuations are defined as [20]

$$C_E(i, t) = \frac{\langle \Delta H_i(t) \Delta H_0(0) \rangle}{\langle \Delta H_0(0) \Delta H_0(0) \rangle}, C_P(i, t) = \frac{\langle p_i(t) p_0(0) \rangle}{\langle p_0(0) p_0(0) \rangle} \quad (2)$$

where  $\Delta H_i(t) \equiv H_i(t) - \langle H_i \rangle$ , and  $\langle \cdot \rangle$  denotes ensemble averages. Note that  $C_{E/P}(i, t=0) = \delta_{i,0}$ . Therefore, the correlation functions  $C_{E/P}(i, t)$  describe the spatiotem-

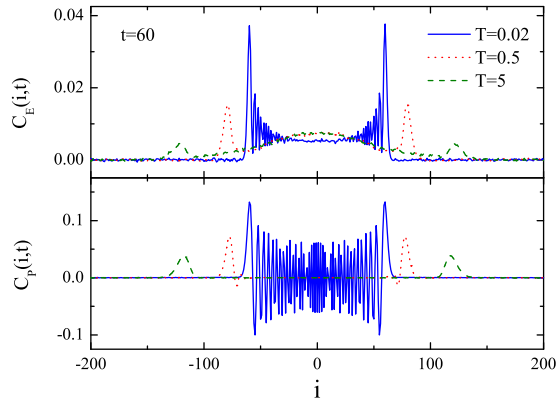


FIG. 1: (color online) Spatial distributions of the correlation functions of  $C_E(i, t)$  (upper panel) and  $C_P(i, t)$  (lower panel) at  $t = 60$  for  $T = 0.02, 0.5$  and  $5$  for the FPU- $\beta$  lattice with  $N = 500$ .

poral spreading of the initial energy/momentum fluctuations [20].

In Fig. 1, we depict the spatial distributions of the correlation functions  $C_{E/P}(i, t)$  at  $t = 60$  for different temperatures. The values  $T = 0.02, 0.5$  and  $5$  correspond to low, intermediate and high temperature regimes, according to the scaling behavior of the aspect ratio  $\epsilon = \langle (q_i - q_{i-1})^4 \rangle / \langle (q_i - q_{i-1})^2 \rangle$ . The aspect ratio scales as  $\epsilon \propto T$  in the low temperature regime and as  $\epsilon \propto T^{1/2}$  in the high temperature regime. As can be seen from Fig. 1, both distributions possess symmetric propagating fronts with identical propagation velocities. These propagating fronts are induced by the fastest travelling energy carriers [19, 20]. With increasing temperature the propagation velocity increases, which is caused entirely by the presence of nonlinear terms in the equations of motion. The fluctuations of  $C_P(i, t)$  are much smaller than those of  $C_E(i, t)$ . Therefore, we will determine the sound velocity  $c_s$  by measuring the peak positions of the propagating fronts for  $C_P(i, t)$ , as in Ref. [20]. We have also tested that the results do not depend on the type of boundary conditions (fixed or periodic).

Let us briefly introduce the predictions of sound velocity for solitons and effective phonons. According to [11, 12], the soliton profile with  $z \sim q_i - q_{i-1}$  is given by

$$Q_s(z) = \sqrt{2(c_s^2 - 1)} \operatorname{sech} \left( 2z \sqrt{(c_s^2 - 1)/c_s^2} \right). \quad (3)$$

It follows that the energy of a soliton is proportional to  $c_s^3 \sqrt{c_s^2 - 1}$ , where we assume  $c_s > 0$  without loss of generality. Using a Boltzmann distribution for energies of excitations, we conclude that the temperature  $T$  introduces an energy scale such that larger soliton energies are exponentially suppressed. At the same time smaller energies imply smaller sound velocities. Therefore a Boltzmann distributed gas of solitons will typically show maximum

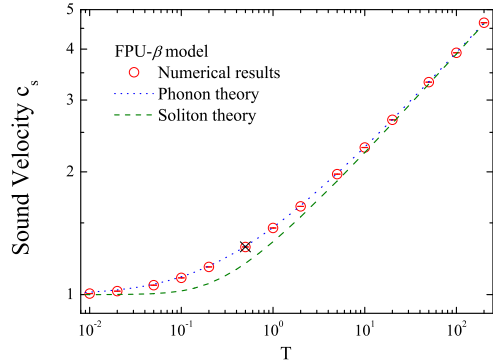


FIG. 2: (color online) Sound velocity  $c_s$  as the function of temperature  $T$  for the FPU- $\beta$  lattice with  $N = 1000$ . The circles are the numerical results. Error bars have been plotted, but they are much smaller than the symbol size. The dotted line is the analytic prediction for effective phonons from Eq. (5) and the dashed line is the analytic prediction for solitons from Eq. (4) with  $\eta = 2.215$ . The numerical result obtained for  $T = 0.5$  in Ref. [20] is plotted with a cross symbol.

sound velocities which correspond to solitons with an energy of the order of the temperature  $T$ . Therefore it follows that [19]

$$c_s^3 \sqrt{c_s^2 - 1} = \eta T. \quad (4)$$

The constant  $\alpha$  is a free fit parameter. Note that  $c_s \rightarrow 1$  as  $T \rightarrow 0$  and  $c_s \approx \eta^{1/4} T^{1/4}$  as  $T \gg 1$  in the high temperature regime.

For the effective phonons, the sound velocity is defined as the maximum group velocity of the renormalized phonons. Here, renormalization implies a mean field treatment of nonlinear terms in the equations of motion. As a result eigenfrequencies of phonons are renormalized, and will increase with increasing temperature. Therefore, renormalized phonons will also yield sound velocities which increase with increasing temperature, becoming supersonic as compared to the case of  $T \rightarrow 0$ . In particular,  $c_s = \partial \hat{\omega}_k / \partial k|_{k=0}$  where  $\hat{\omega}_k = 2\sqrt{\alpha} \sin k/2$  with  $0 \leq k < 2\pi$  and  $\alpha = 1 + \langle \sum_i (q_i - q_{i-1})^4 \rangle / \langle \sum_i (q_i - q_{i-1})^2 \rangle$  [17]. It follows [17]

$$c_s = \left( 1 + \frac{\int_0^\infty x^4 e^{-(x^2/2+x^4)/T} dx}{\int_0^\infty x^2 e^{-(x^2/2+x^4)/T} dx} \right)^{\frac{1}{2}}. \quad (5)$$

For  $T \rightarrow 0$  we find  $c_s \rightarrow 1$ , and in the high temperature region  $c_s \approx \sqrt{\int_0^\infty x^4 e^{-x^4/4T} dx / \int_0^\infty x^2 e^{-x^4/4T} dx} \approx 1.22T^{1/4}$ . Both predictions (solitons and phonons) yield three similar results for the sound velocity: (i)  $c_s \geq 1$ ; (ii)  $c_s(T \rightarrow 0) \rightarrow 1$ ; (iii) in the high temperature regime, the sound velocities exhibit the same scaling with temperature as  $c_s \propto T^{1/4}$ .

In Fig. 2, we plot the numerically determined sound velocity  $c_s$  as the function of temperature  $T$  for the FPU-

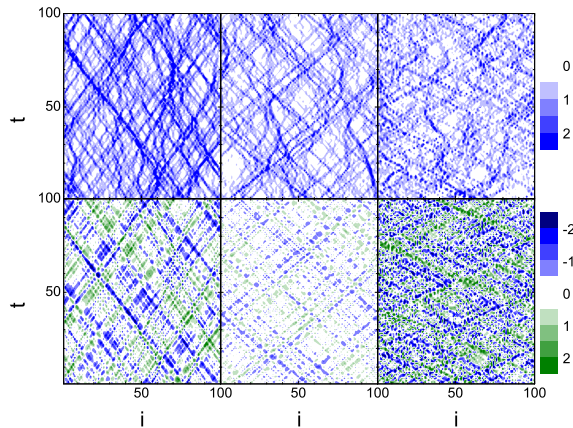


FIG. 3: (color online) Spatiotemporal evolution of energy densities  $H_i(t)/T$  (upper panels) and relative displacements  $q_i(t) - q_{i-1}(t)$  (lower panels) at thermal equilibrium. The left, middle and right columns correspond to the harmonic lattice at  $T = 1$ , and the FPU- $\beta$  lattice at  $T = 1$  and  $T = 20$ , respectively. The lattice size  $N = 100$  and periodic boundary conditions are applied.

$\beta$  lattice. The computational errors are extremely small and  $c_s$  is measured very accurately. The numerical results are compared with the predictions for solitons from Eq. (4), and for effective phonons from Eq. (5). Excellent agreement has been observed for the effective phonon result in the entire temperature region being explored. The soliton curve corresponds to  $\eta = 2.215$ , which reproduces the correct high temperature result. However, the deviation from the prediction for solitons of Eq. (4) is quite distinct in the intermediate temperature regime where  $0.05 \leq T \leq 2$ . We note that variations and optimizations of  $\eta$  do not improve this discrepancy. The cross symbol in Fig. 2 represents the sound velocity  $c_s = 1.31$  measured at  $T = 0.5$  in Ref. [20]. Although it was originally viewed as an evidence for soliton transport, the numerical result is actually coinciding both with our numerical data and with the effective phonon results, in contrast to the soliton theory. This finding provides strong evidence that the effective phonons, rather than the solitons, should be the energy carriers responsible for anomalous transport in the FPU- $\beta$  lattice.

To visualize the energy transport processes, in Fig. 3 we plot the spatiotemporal evolutions of local energy densities  $H_i(t)/T$  and the relative displacement  $q_i(t) - q_{i-1}(t)$  for the harmonic lattice and the FPU- $\beta$  lattice, respectively. The systems are thermalized at a given temperature and then the heat bath is removed. The evolution functions are recorded at thermal equilibrium and results for a suitable time window are displayed. The spatiotemporal patterns for both the FPU- $\beta$  lattice and the harmonic lattice are qualitatively similar. Since solitons are definitely excluded for the harmonic lattice, there appears to be no signature for soliton transport in the FPU- $\beta$  lattice as well. The qualitative behavior of the

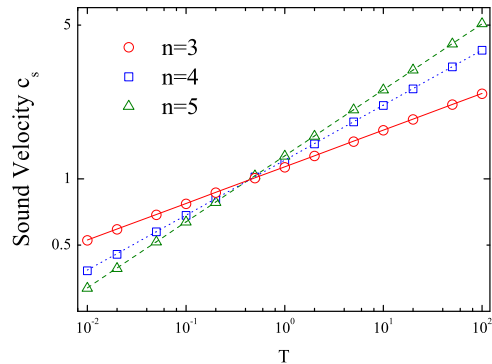


FIG. 4: (color online) Sound velocity  $c_s$  as the function of temperature  $T$  for the  $H_n$  models with  $n = 3, 4$  and  $5$ . The symbols correspond to the numerical results at  $N = 1000$ , whereas the lines are the predictions for effective phonons from Eq. (7). The errors are much smaller than the symbols.

spatiotemporal evolutions does not change for larger time windows.

In the high temperature limit, the FPU- $\beta$  model can be reduced to an  $H_n$  model with  $n = 4$  assuming the following Hamiltonian

$$H_n = \sum_{i=1}^N \left[ p_i^2/2 + |q_i - q_{i-1}|^n/n \right]. \quad (6)$$

To demonstrate the power and consistency of the effective phonon formulation, we consider three different cases with  $n = 3, 4$  and  $5$ . Following the same procedure as for FPU- $\beta$  lattice, the sound velocities of effective phonons can be expressed with a compact formula

$$c_s = [\Gamma((n+1)/n)/\Gamma(3/n)]^{1/2} (nT)^{1/2-1/n} \quad (7)$$

These predictions are plotted in Fig. 4 and compared with numerical results. We again find quantitative agreement for all three models.

Let us discuss some details in the spatiotemporal dependence of the correlation functions. In Fig. 1, the distribution functions of  $C_{E/P}(i, t)$  show many peaks between the two propagating fronts at  $T = 0.02$ . These peaks are typical for coherent phonon propagation in harmonic lattices. For  $T = 0.5$  and  $5$ , there are no visible additional peaks for both distributions and a big hump emerges in the interior region for  $C_E(i, t)$ . The disappearance of the intermediate peaks can be therefore attributed to relaxation processes. Indeed, the distribution functions  $C_{E/P}(i, t)$  for  $T = 0.5$  at various spreading times  $t = 10, 30, 50$  and  $70$  in Fig. 5 show that the short time behavior at  $T = 0.5$  is similar to that for  $T = 0.02$ . The phonon modes relax faster at higher temperatures, while on the other hand, the long wavelength phonon modes possess very long correlation times even at very high temperatures. According to Ref. [20],

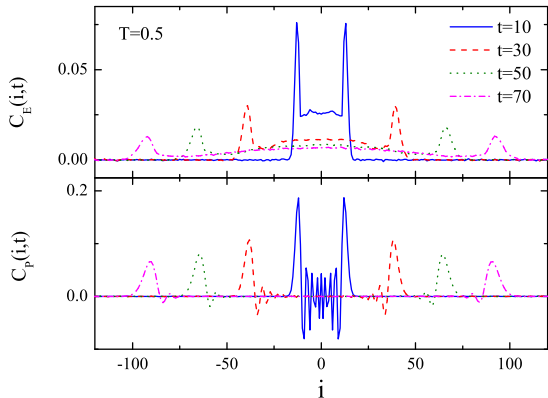


FIG. 5: (color online) Spatial distributions of the correlation functions of  $C_E(i, t)$  (upper panel) and  $C_P(i, t)$  (lower panel) at  $T = 0.5$  for various values of time  $t = 10, 30, 50$  and  $70$ , for the FPU- $\beta$  lattice with size  $N = 500$ .

the correlation function of energy fluctuations  $C_E(i, t)$  is nothing but the energy density probability distribution function (PDF). Therefore we can study the energy diffusion process by measuring the mean square displacement (MSD) as  $\langle r^2(t) \rangle = \sum_i i^2 C_E(i, t)$ . For PDFs shown in Fig. 5, the MSD is dominated by the area around the propagating fronts and can be approximated as  $\langle r^2(t) \rangle \propto t^{2-\nu}$  where the exponent  $\nu$  characterizes the diminishing of the peak area with time as a consequence of slow but unavoidable dephasing of even long wave length phonons. According to [20] the exponent

$0 < \nu < 1$ , and therefore the diffusion process is superdiffusive as  $\langle r^2(t) \rangle \propto t^\sigma$  with  $\sigma = 2 - \nu$ . It is interesting to analyze the connection between superdiffusion and anomalous heat conduction for the FPU- $\beta$  lattice. Recall that the heat flux of phonons is  $J_k = v_k E_k$  [2] where  $k$  denotes the wave number. The correlation function of the total heat flux ( $J = \sum_k J_k$ ) can be approximately obtained as  $\langle J(t)J(0) \rangle \approx \langle c_s^2 E_0(t)E_0(0) \rangle \propto t^{-\nu}$  since the only long time correlation is due to the energy carried by the long wave-length phonon modes. Applying the Green-Kubo formula for heat conductivity [2], we obtain  $\kappa \propto \int_0^{N/c_s} \langle J(t)J(0) \rangle dt \propto N^\beta$  where  $\beta = 1 - \nu$ . Without knowing the exact value of  $\beta$  and  $\sigma$ , we obtain that the superdiffusion and anomalous heat conduction are connected via the exponent relation  $\beta = \sigma - 1$  [20, 22].

In conclusion, we have investigated the energy transport processes for the FPU- $\beta$  lattice using an equilibrium approach. To identify the energy carriers, we accurately measure the sound velocity of the energy carriers by following the correlated spreading of the initial energy/momentum fluctuations. The sound velocities are found to be in excellent agreement with theoretical predictions for effective phonons. This predicability has been further confirmed for a series of  $H_n$  models. On the other hand, no signature of soliton transport has been detected by visualizing the spatiotemporal evolutions of local energy densities and relative displacements. Therefore our numerical results clearly reveal that the energy carriers are long wavelength phonons for the FPU- $\beta$  lattice.

We thank J. D. Bodyfelt, Ch. Skokos, D. O. Krimer and T. Lapteva for useful discussions.

- 
- [1] F. Bonetto, J. L. Lebowitz, and L. Ray-Bellet, in *Mathematical Physics 2000*, edited by A. Fokas, A. Grigoryan, T. Kibble, and B. Zegarlinski (Imperial College Press, London, 2000), pp. 128-150.
- [2] S. Lepri, R. Livi, and A. Politi, Phys. Rep. **377**, 1 (2003).
- [3] A. Dhar, Adv. Phys. **57**, 457 (2008).
- [4] J.-S. Wang, J. Wang, and J. T. Lü, Eur. Phys. J. B, **62**, 381 (2008).
- [5] S. Lepri, R. Livi, and A. Politi, Phys. Rev. Lett. **78**, 1896 (1997).
- [6] G. Zhang and B. Li, J. Chem. Phys. **123**, 114714 (2005).
- [7] N. Yang, G. Zhang, and B. Li, Nano Today (2010).
- [8] C. W. Chang, D. Okawa, H. Garcia, A. Majumdar, and A. Zettl, Phys. Rev. Lett. **101**, 075903 (2008).
- [9] A. Pereverzev, Phys. Rev. E **68** 056124 (2003).
- [10] K. Aoki, J. Lukkarinen, and H. Spohn, J. Stat. Phys. **124**, 1105 (2006).
- [11] J. A. D. Wattis, J. Phys. A **26**, 1193 (1993); G. Friesecke and J. A. D. Wattis, Commun. Math. Phys. **161**, 391 (1994).
- [12] F. Zhang, D. J. Isbister, and D. J. Evans, Phys. Rev. E **61**, 3541 (2000); F. Zhang, D. J. Isbister, and D. J. Evans Phys. Rev. E **64**, 021102 (2001).
- [13] S. Flach and C. R. Willis, Phys. Rep. **295**, 181 (1998); S. Flach and A. V. Gorbach, Phys. Rep. **467**, 1 (2008).
- [14] C. Alabiso, M. Casartelli, and P. Marenzoni, J. Stat. Phys. **79**, 451 (1995); C. Alabiso and M. Casartelli, J. Phys. A: Math. Gen. **34**, 1223 (2001);
- [15] S. Lepri, Phys. Rev. E **58**, 7165 (1998).
- [16] B. Gershgorin, Y. V. Lvov, and D. Cai, Phys. Rev. Lett. **95**, 264302 (2005); B. Gershgorin, Y. V. Lvov, and D. Cai, Phys. Rev. E **75**, 046603 (2007).
- [17] N. Li, P. Tong, and B. Li, Europhys. Lett. **75**, 49 (2006); N. Li and B. Li, Europhys. Lett. **78**, 34001 (2007).
- [18] D. He, S. Buyukdagli, and B. Hu, Phys. Rev. E **78**, 061103 (2008).
- [19] K. Aoki, and D. Kusnezov, Phys. Rev. Lett. **86**, 4029 (2001).
- [20] H. Zhao, Phys. Rev. Lett. **96**, 140602 (2006).
- [21] B. Li, J. Wang, L. Wang, and G. Zhang, Chaos **15**, 015121 (2005).
- [22] S. Denisov, J. Klafter, and M. Urbakh, Phys. Rev. Lett. **91**, 194301 (2003).
- [23] H. Zhao, Z. Wen, Y. Zhang, and D. Zheng, Phys. Rev. Lett. **94**, 025507 (2005).